

Estimate of Water Residence Times in Tudor Creek, Kenya Based on Sea Surface Heat Fluxes and Observations of the Horizontal Temperature Gradient During Different Seasons

Nguli M. M.¹, Rydberg L.² and Francis, J.³

¹Kenya Marine & Fisheries Research Institute, Box 81651, Mombasa, Kenya; ²University of Gothenburg, Earth Sciences Centre, Oceanography, Box 460, SE-405 30 Göteborg, Sweden; ³University of Dar es Salaam, Faculty of Aquatic Science and Technology, Box 35060, Dar es Salaam, Tanzania

Key words: Kenya, water exchange, sea surface heat fluxes, heat budget, Kenya coastal meteorology

Abstract—Salinity and temperature measurements were carried out in Tudor Creek, Kenya from 1995–98 in order to determine water exchange between the creek and the adjacent Indian Ocean. Data from the Kenya Meteorological Department including gauging data from two small rivers were employed to estimate long-term rainfall, evaporation and river runoff. However, even though the observed salinity gradient in the creek appeared consistent with dry and rain periods, estimates of river runoffs were not good enough to calculate water exchange, based on salt conservation. Runoff in general was also too small to give reliable rating curves (correlation between rainfall and river runoff). For this reason, heat conservation was used for the calculation of water exchange. Although estimates of sea surface heat fluxes were based on coarse global climatology data with large seasonal variations in the net heat flux (from 50–150 Wm⁻²), the result was surprisingly consistent, with similar water exchange during all different seasons. Residence times for the creek waters in relation to the ocean water are between 3–5 days, 5 days for the waters inside the deep inlet. During spring tides, the exchange is about twice as large as during neap tides.

INTRODUCTION

The water exchange and circulation, and thus the exchange of properties between a coastal embayment and the offshore ocean waters, are due to a number of factors, mainly the freshwater input and the tides. Additional factors include winds, external barotropic and baroclinic motions and heat input. Also, the topography of the bay itself and particularly its inlet is of major importance (see e.g. Stommel and Farmer, 1953; Nunez Vaz *et al.*, 1989).

The role of the tide is to drive a strong diffusive exchange, usually such that the waters are well mixed from surface to bottom and the flow is

barotropic during most of the tidal cycle. In quite a few estuaries, however, the net freshwater input, i.e. the sum of precipitation, evaporation and river runoff, creates a flow of low saline water on top of the denser ocean water, resulting in a stratified environment and a two-layer estuarine circulation. In Kenya though, most coastal embayments (which are locally termed creeks) experience relatively small freshwater inputs, which are rapidly mixed with the oceanic water by tides. Therefore, the creeks normally appear as well-mixed, and may be classified as “coastal plain estuaries”, *sensu* Pritchard. Exceptions may occur during periods of intensive rains. This paper deals with estimates of the water exchange in Tudor Creek, one of

several shallow tidal estuaries on the Kenya coast (Fig. 1 and 2).

To date, there exist only a few studies of hydrography and water circulation of Kenyan creeks. Analyses of tides include those by Pugh (1979) in Kilindini Harbor, Magori (1998) in Mtwapa Creek and Nguli (1994) and Odido (1994) in Tudor Creek. All sites are in the Mombasa area (Fig. 1 and 2). Analyses of salinities, temperatures and currents have been conducted by Norconsult (Anon, 1975), also in the Mombasa waters and by Kitheka (1997) in Gazi Bay, further south on the

coast (Fig. 1). In his PhD thesis, Nguli (2006) gives an overview of the hydrography of some Kenyan creeks and the adjoining coastal waters, providing data on salinities, temperatures, currents and sea levels from Gazi Bay and Tudor and Kilifi Creeks. In this paper we focus on the Tudor Creek, from which the best set of data was obtained.

Seasonal mean salinities and temperatures are calculated from approximately bi-monthly hydrographic surveys in the Tudor Creek for a period of about 3 years, from 1995-98. River discharge and evaporation is estimated from Kenya

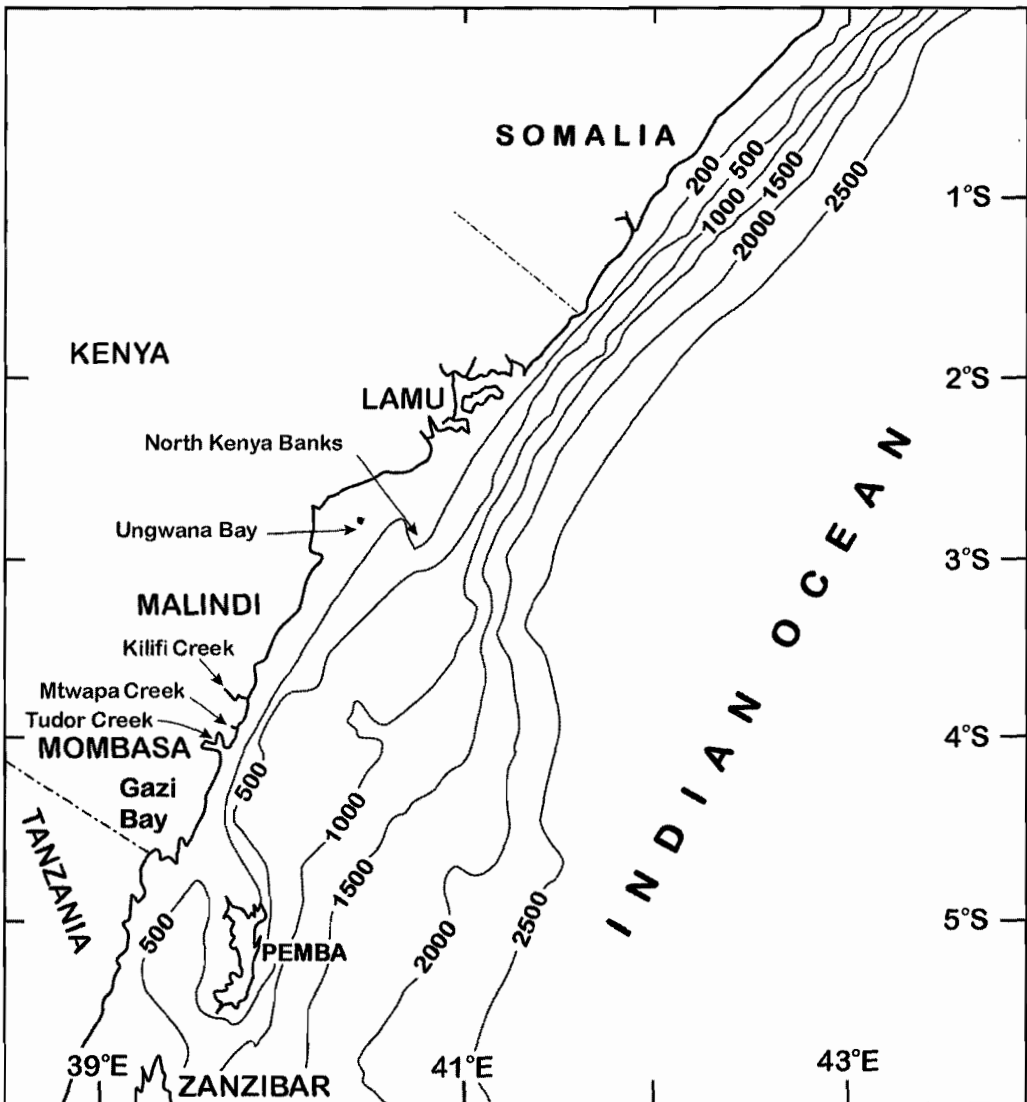


Fig. 1. The Kenya coast with its narrow continental shelf and sites mentioned in the text

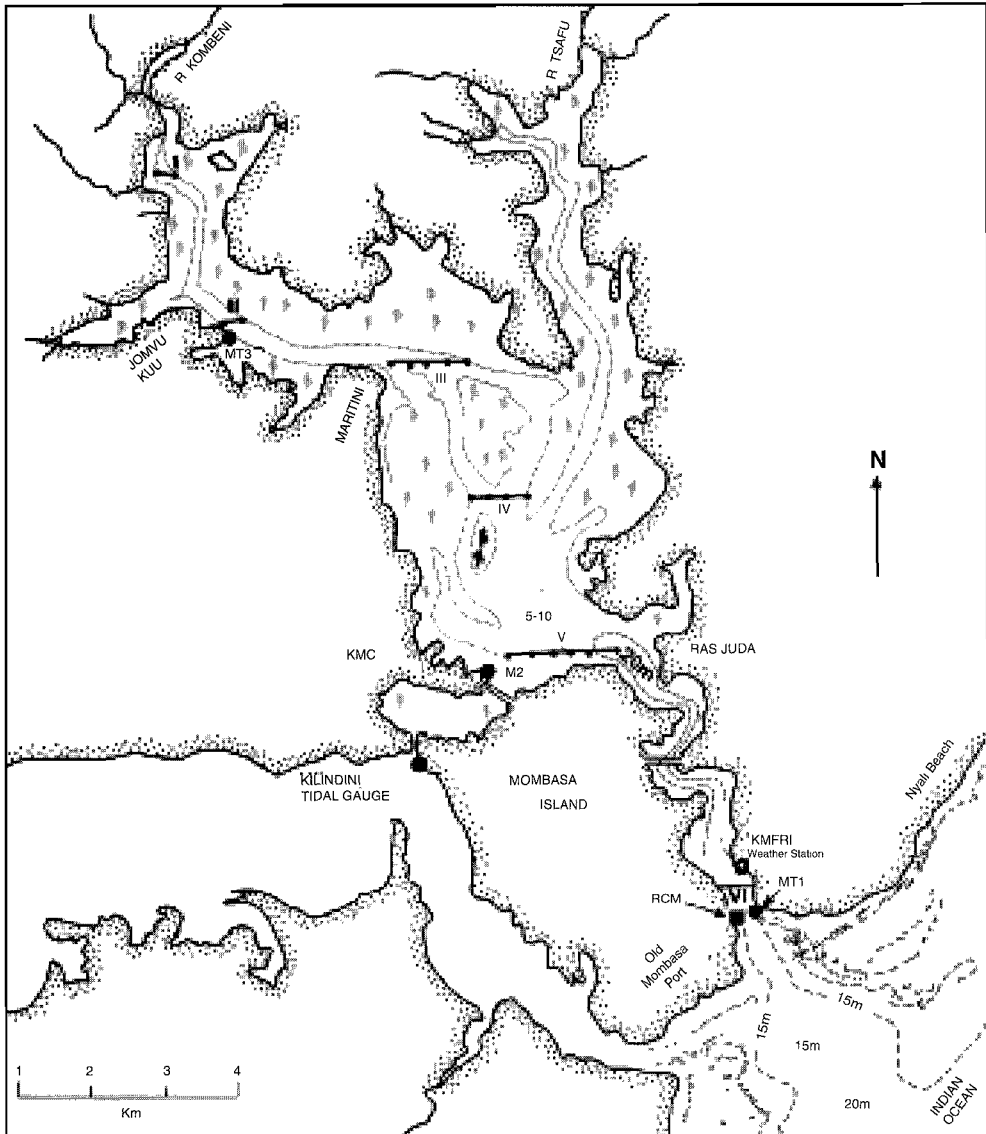


Fig. 2. Map of Tudor Creek, showing sections for hydrographic surveys (salinity and temperature; Stns I-IV), positions for tide gauge (MT1-3) and recording current meter deployments (RCM) and for the site of the weather mast (KMFRI)

Meteorological Department station data on rainfall, amongst others. Calculations of water exchange are based on heat and salt conservation, applied during periods of dry and wet climate, respectively. Global web-based data are employed for estimates of long term mean sea surface heat fluxes. These are compared to data obtained from a weather mast, positioned adjacent to the creek, and are also used for water exchange calculations.

STUDY SITE AND DATA

The Tudor Creek is located in the equatorial zone between latitude $03^{\circ} 40' S$, and $04^{\circ} 00' S$ and is the northern branch of the creek waters surrounding Mombasa Island (Fig. 2). The creek has a long and deep inlet (average about 20 m) connecting the much shallower inner bay to the open ocean. Two seasonal rivers, Kombeni and Tsalu Rivers, are draining an area of 550 km^2 (450 and 100 km^2 ,

respectively). Norconsult (Anon, 1975) estimated the average freshwater discharge from these rivers to be $0.9 \text{ m}^3\text{s}^{-1}$ with a maximum of $1.8 \text{ m}^3\text{s}^{-1}$ from April-June. The tidal range at the entrance is 3.2 m at spring and 1.1 m at neap (Admiralty Tide Tables). Outside the entrance, there is a 2-3 km wide opening in the fringing coastal reef. The sill depth in this section is 12-14 m at spring low water (LWS).

The shallow inner basin is fringed by mangroves and mudflats (Fig. 2). The basin has an area of 6.37 km^2 at LWS and 22.35 km^2 at HWS. Mangrove forests, as indicated in figure 2 occupy some 8 km^2 . The sea surface area of the inlet, on the other hand, is small varying from 1.31 km^2 at LWS to 1.72 km^2 at HWS (see also Table 1).

Table 1. Volumes and areas of Tudor Creek (including the inlet) at different stages of the tide. The mean depth (row 5) is similar because the relative proportion of the deep inlet increases at low water, when the volume of the inner basin is small

	MHWS	MHWN	MLWN	MLWS
Sea level (datum ref)	3.5	2.4	1.3	0.3
Surface area (km^2)	24	14	11	7.5
Volume ($\times 10^6 \text{ m}^3$)	95	68	54	41
Mean depth (m)	5	5	5	5.5

Field studies in Tudor Creek took place from 1995-98. These consisted of hydrographic surveys, basically mapping salinities and temperatures every second month. In total, 21 such surveys, covering all seasons were carried out. The distribution of stations is shown in figure 2. Data were collected from several depths, using a salinity-temperature sensor of type Aanderaa 3210. Current measurements with self-recording current meters and pendulum current meters were carried out in the inlet (Stn RCM). For a period of one month, three tide gauges were deployed simultaneously at Stns MT1-3 (Fig 2). At Stn KMFRI, an Aanderaa weather mast was erected. Weather mast observations were carried out from 14 June-28 August 1996. The mast was equipped with sensors for measurements of air temperature, air pressure, humidity, wind speed and direction, cloud cover, solar and net radiation. Sea surface temperature and salinity were measured in addition, using a free

floating sensor, connected through a cable to the weather mast data logger. Mast data were recorded every 20 minutes. These data are used here to estimate sea surface heat fluxes.

The present study also employs meteorological data from several coastal stations belonging to the Kenya Meteorological Department (KMD). These data are used in order to estimate river discharge into Tudor Creek. Mombasa Airport Meteorological Station is the main station on the coast. It delivers daily observations at 0600 and 1200 GMT. Data from the airport comprises wind speed and direction, temperature, relative humidity, cloud cover, solar radiation, rainfall and evaporation from the period 1958-97. Data from other stations along the coast were employed in order to improve estimates of coastal rainfall and evaporation and to evaluate local variations in relation to the runoff figures. All data sets which are used here originate from KMD yearbooks (i.e. Anon, 1996a; 1997) such as rainfall and evaporation data from Msambweni for 1955-97, Ramisi for 1966-97, Kikoneni for 1972-97, Shimba Hills for 1975-97, Shimoni for 1957-97 and Malindi Airport for 1962-97 (for positions and details, see Nguli, 2006).

There are no observations of river discharge into Tudor Creek. In fact, several smaller rivers discharge into the ocean along the southern coast of Kenya, but only one, the Mkurumudzi River, entering into Gazi Bay (Fig. 1), has been gauged for longer times (Anon, 1996b). In addition, some research data are available from Pemba River (Anon, 1975), which discharges into Kilindini Harbor to the south of Mombasa Island. The data from Mkurumudzi and Pemba Rivers are employed together with the aforementioned meteorological data, in order to establish a rating curve for the river runoff into Tudor Creek.

Most data are averaged on a long term mean monthly (climatology) basis. A further averaging to "mean seasonal data" is based on the assumption that the Kenya coast experiences four rather distinct seasons (Nguli, 2006), with climate shifting from wet to dry and from cold to warm. These are the Inter Monsoon Long Rain (IMLR, April-May), the South West Monsoon (SWM, June-Sept), the Inter Monsoon Short Rain (IMSR, Oct-Nov) and the North East Monsoon (NEM,

Dec-March) season, respectively. Of these, the NEM is the driest period and the IMLR is the wettest.

THEORY

Salt and volume conservation

Volume and salt conservation in an estuary is known as Knudsen’s hydrographical theorem, (Knudsen, 1899). Figure 3 indicates a simple model for water exchange (q_f, q_o) in relation to the net freshwater supply, and the mean salinities of estuarine and ocean water, S_o and S_1 .

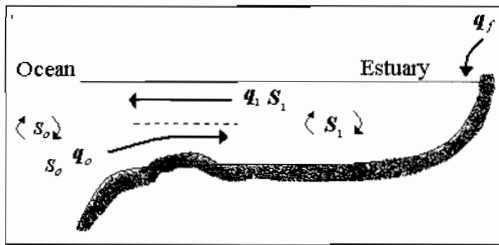


Fig. 3. The figure indicates an ideal, well-mixed estuary, where S_1 is the estuarine mean salinity and S_o is the oceanic salinity. The fluxes q_f and q_o represent the corresponding water exchange of “water with salinities S_1 and S_o ”, respectively

In a steady state, as employed by Knudsen, the continuity equations for volume and salt are;

$$q_f = q_1 - q_o \quad q_1 S_1 = q_o S_o \dots\dots\dots \text{Eq. 1 a,b}$$

The volume fluxes, q_1 and q_o are the fluxes of water with salinity S_1 and S_o , respectively. The net freshwater supply is;

$$q_f = q_r - q_p - q_e \dots\dots\dots \text{Eq. 1c}$$

where q_r is the river discharge, q_p is the precipitation on the estuarine surface, and q_e is the evaporation. From the above equations, we obtain the influx of ocean water as;

$$q_o = \frac{q_f S_1}{\Delta S} \dots\dots\dots \text{Eq. 2}$$

where $\Delta S = S_o - S_1$. With known salinities and net freshwater supply, the water exchange (q_o) can be determined from Eq. 2. Arons and Stommel (1951) investigated the salinity gradient along the longitudinal section of a well mixed estuary using the following balance;

$$u \frac{\partial S}{\partial x} = \frac{\partial}{\partial x} \left(K_x \frac{\partial S}{\partial x} \right) \dots\dots\dots \text{Eq. 3}$$

The authors used the so called “Reynolds analogy” introducing a length scale, i.e. the length of the estuary, L (over which the salinity difference is ΔS), to obtain an expression for the eddy diffusivity;

$$K_x = q_o \frac{L}{A_v} \text{ Here, } A_v \text{ is the cross-section area. Thus, we obtain;}$$

$$u_f S_1 = K_x \frac{\Delta S}{L} \text{ or } \frac{q_f}{A_v} S_1 = K_x \frac{\Delta S}{L} \dots\dots\dots \text{Eq. 4 a, b}$$

Thus, the eddy diffusivity, K_x can be calculated indirectly from the survey data. The water exchange (q_f, q_o) is sometimes expressed in terms of residence time. The residence time for the estuarine water of salinity is (for $q_f \ll q_o$);

$$T_r = \frac{V}{q_1} \cong \frac{V}{q_o} \dots\dots\dots \text{Eq. 5}$$

Here, V is the volume of the estuary. Therefore, for the estuarine water, Eq. 5 is exact only for q_1 but approximate for the ocean water exchange.

The equation for conservation of heat may be expressed in a similar way to that for salinity (Eq 3). In addition, there is an additional source term, the net flux of heat through the sea surface, Q_{am} . Thus;

$$\rho C_p \bar{h} \left(u_f \frac{\partial T}{\partial x} - K_x \frac{\partial^2 T}{\partial x^2} \right) = Q_{am} \dots\dots\dots \text{Eq. 6}$$

Here, ρ is the seawater density and C_p is the heat capacity for seawater, T is temperature and K_x is the horizontal eddy diffusivity, assumed similar for heat and salt. The velocity u is an ensemble mean (following the Reynolds analogy), representing the net freshwater velocity ($u_f = q_f/A_v$). The equation (see e.g. Gill 1982), assumes a steady state where \bar{h} is the mean depth over which Q_{am} is distributed. An integrated, simplified version of Eq. 6, where the heat transport by the net freshwater velocity is assumed negligible reads;

$$\rho C_p q_o \Delta T = A_h Q_{am} \dots\dots\dots \text{Eq. 7}$$

Here, ΔT is the temperature difference between the creek and the ocean and A_h is the horizontal area of the creek. The water exchange is $q_o = q_1$ (when q_f is negligible). Thus, we assume that turbulent, diffusive transport of heat is much more efficient than advective transport by the mean flow.

The net sea surface heat flux can be estimated from the following simplified expression (e.g., Gill, 1982);

$$Q_{atm} = Q_s - Q_b - Q_e - Q_h \dots\dots\dots \text{Eq. 8}$$

Q_s is the short wave solar radiation, entering through the sea surface (the incident radiation, Q_{si} reduced for surface albedo), Q_b is the net long wave back radiation from the sea surface, Q_e is the latent heat flux at the sea surface, and Q_h is the sensible heat flux or direct conduction through the sea surface.

The turbulent heat fluxes, Q_e and Q_h , are derived from bulk formulas, based on observed meteorological data, i.e. wind speed, W , air temperature, T_a , sea surface temperature, T_s and relative humidity, r_h . In their most common form they may be written as

$$Q_h = \rho_a C_p C_i (T_s - T_a) W \dots\dots\dots \text{Eq. 9}$$

$$Q_e = \rho_a L_v C_e (q_s - q_a) W \dots\dots\dots \text{Eq. 10}$$

In Eq. 9, C_p is the specific heat of air at constant pressure, P and C_i is the Stanton number, a non-dimensional transfer coefficient, of the order 10^{-3} , while ρ_a is the air density. In Eq. 10, q_a is the specific humidity of air (mass of water per unit mass of air) at the standard level (normally 10 m) and q_s is the saturation humidity at the sea surface.

The relative humidity, $r_h = (q_s/q_a)$. Thus, $q_a = (0.62197e_a)/(P-0.37e_a)$ and $q_s = (0.62197)e_w/(P-0.378e_w)$

where e_a is the vapor pressure of the air and e_w is the saturation vapor pressure. L_v is the latent heat of vaporisation and C_e is a transfer coefficient, the Dalton number, also of the order of 10^{-3} . L_v and C_p are calculated from the following expressions

$$L_v = 4.1868(597.31-0.56525T_a) \times 10^{-3} \text{ and } C_p = 1004.6(1-0.8375q_a).$$

There is no general consensus on the empirical eddy exchange coefficients, C_i and C_e . Field studies have shown that they may vary with wind speed and atmospheric stability. Friehe and Schmitt (1976) and Large and Pond (1981; 1982) derived relatively simple but apparently robust expressions (Gill, 1982; Taylor 2000). Since then, several different transfer coefficients schemes of varying complexity and sophistication have been proposed. In order to calculate Q_h and Q_e from the mast data, we adopted a more elaborated scheme, following Mohanty and Mohan Kumar (1990) and Mohanty

et al. (1996). This was developed for tropical waters. Here, both wind speed and stability are taken into account.

RESULTS

This section contains a short presentation and a preliminary analysis of coastal meteorology data obtained from KMD, particularly solar radiation, evaporation and rainfall. Rainfall and evaporation climatology (i.e. long-term monthly mean) are used for establishment of rating curves and for further estimates of river discharge and net freshwater supply into the Tudor Creek. Solar radiation data is employed for comparison with weather mast observations and with global web data. Weather mast data are used to calculate net sea surface heat fluxes. Global web data are used for the same purpose. Finally we show the seasonal distribution of salinities and temperatures in the Tudor Creek, based the hydrographic surveys, and present calculations of water exchange based on salt and heat conservation.

Climatology from coastal meteorological stations

Evaporation

Interpolation of individual station data (see next section, Precipitation) was used to obtain the long-term monthly mean evaporation in three different catchment areas, comprising the rivers entering Gazi Bay, Tudor and Kilifi Creeks. The results are shown in figure 4. Kilifi and Tudor Creek catchments areas feature higher evaporation rates, 170-180 mm/month, than Gazi Bay in the south, with an average 140 mm/month.

Precipitation

Monthly mean precipitation was calculated for catchment areas and by interpolating available station data. For the Gazi Bay catchment area, four stations (Msambweni, Ramisi, Kikoneni and Shimba Hills) were employed. Data for the Tudor Creek were based on Mombasa Airport and Gede data. For Kilifi finally, Malindi and Mombasa data were used. The data were weighted manually to fit with the catchments areas. Long term mean precipitation rate, p and total catchment area

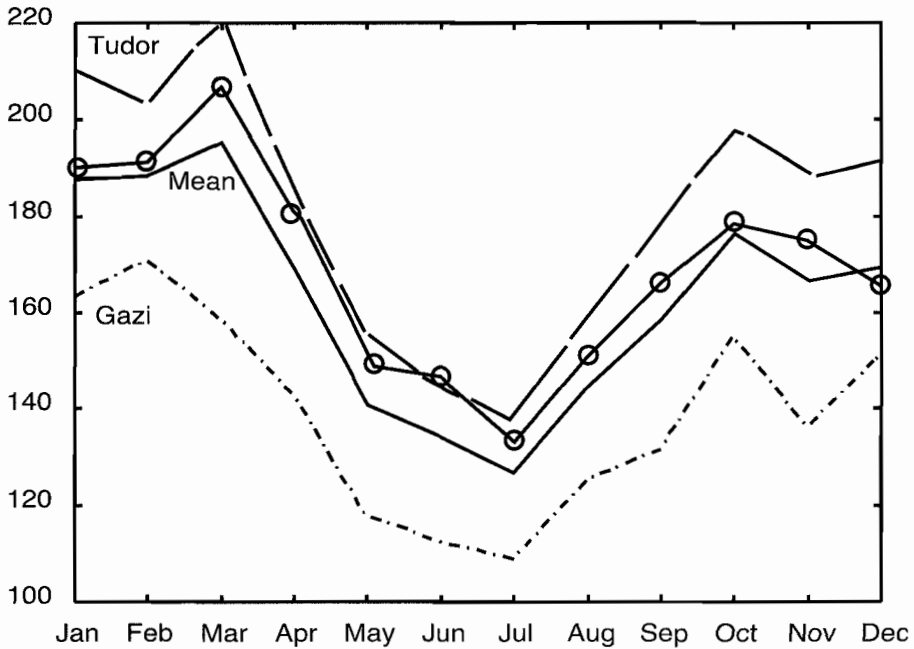


Fig. 4. Long term monthly mean evaporation (mm/month) in catchment areas for Gazi Bay, Tudor and Kilifi Creeks for the period 1958-97 (Raw data from KMD)

precipitation P is shown in Table 2, the monthly mean precipitation also in figure 5.

In order to indicate the year to year variability, monthly precipitation at Mombasa Airport is shown separately in figure 6 for the period 1987-97. Precipitation during the years of hydrographic observations is highlighted in the figure. The bimodal pattern, with maximum rainfall in April-May (IMLR) and in Oct-Nov (IMSR) is obvious both in figure 5 and 6. However, although the long term mean rainfall seem consistent, indicating

minor but probably correct differences in onset of monsoon rains and monthly rainfall (Fig. 5; Table 2), figure 6 data shows that rainfall varies highly from one year to another. Of particular interest is the wet year of 1997. The year featured a total rainfall of 2,175 mm, twice a normal year, coinciding with an extraordinary strong El-Nino.

Solar radiation

Solar radiation is observed at Mombasa and Malindi Airports. Malindi at latitude $03^{\circ} 14'S$

Table 2. Long term monthly mean precipitation rate within the river catchment area, p (mm/month) and total catchment area precipitation, P (m^3s^{-1}). The catchment areas are, for Gazi Bay $200 km^2$, for Tudor Creek $550 km^2$ and for Kilifi $1700 km^2$ (Data are from KMD)

AREA	JAN	FEB	MAR	APR	MAY	JUN	JUL	AUG	SEP	OCT	NOV	DEC	MEAN
Gazi, p	19.9	12.9	65.3	201.6	234	79.1	74.9	82.4	49.9	187	127	84.4	101.5
P	1.49	0.96	4.88	15.05	17.51	5.91	5.60	6.15	3.73	14.00	9.48	6.30	7.6
Tudor, p	23.8	12.7	57.9	167	285	61.9	65.8	72	53.4	185	120.4	85	109.2
P	4.89	2.61	11.89	34.29	58.52	12.71	13.51	14.78	10.96	37.98	24.72	17.45	20.3
Kilifi, p	21.4	20.8	52.9	167	277	119	90.9	81.5	63.7	129.5	107.7	66.5	100
P	13.98	13.59	34.56	109.11	180.9	77.75	59.39	53.25	41.62	84.61	70.37	43.45	120.2

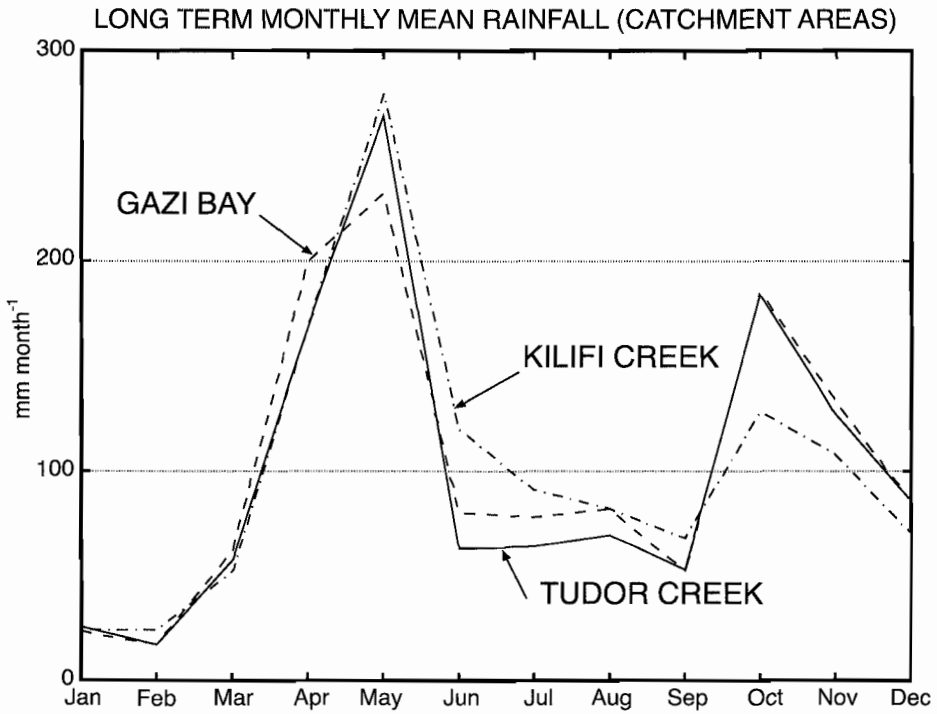


Fig. 5. Long term monthly mean rainfall in catchment areas for Gazi Bay, Tudor and Kilifi Creeks for the period 1958-97 (Raw data from KMD)

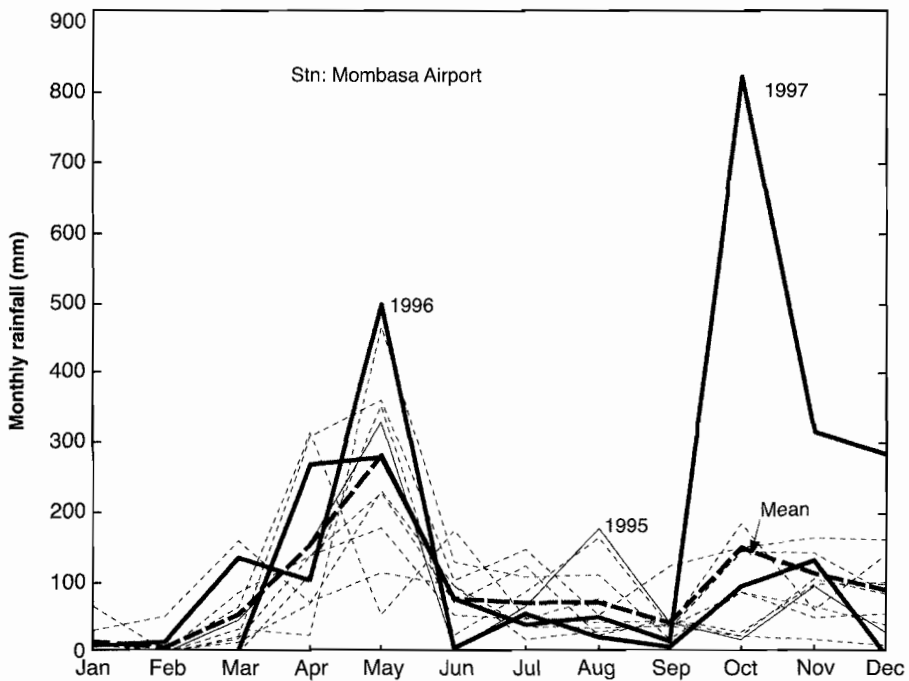


Fig. 6. Eleven years of monthly precipitation (1987-97) at Mombasa Airport, highlighting the years of hydrographic observations in Tudor Creek, 1995-97 (Raw data from KMD)

longitude 40° 06'E is situated 120 km north of Mombasa (Fig. 1). Long-term monthly mean incident solar radiation, Q_{si} (see text in connection with Eq. 8) at these stations is shown in figure 7. The incident radiation is higher at Mombasa Airport than in Malindi. May-July data are similar (180 Wm^{-2}), but otherwise the difference between the two stations is substantial. From October to March the values in Mombasa are 240-250 Wm^{-2} and in Malindi 220-230 Wm^{-2} . Judging from rainfall data (Fig. 5) where the northern coast (Kilifi data) has less rain, one would expect the opposite situation.

River runoff calculated from precipitation

Mkurumudzi River, entering Gazi Bay was gauged occasionally from 1966-87 (Anon, 1996b). In all, there are 67 observations available, at more or less arbitrary dates, but fairly well distributed over seasons. The gauging data from Mkurumudzi River were put together as shown in Table 3, showing periodic and long term monthly mean runoff.

Runoff from the Mkurumudzi River was used in combination with the precipitation rates, p in the catchment areas of Gazi Bay, to obtain a

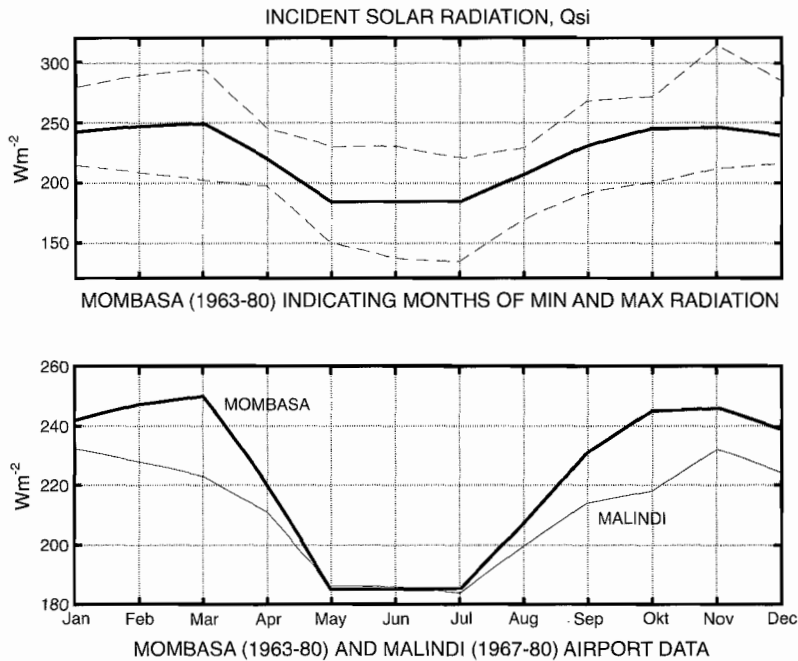


Fig. 7. Long term monthly mean incident solar radiation, Q_{si} , at Mombasa Airport, indicating maxima and minima during the period of observations (upper panel) and Mombasa and Malindi Airports (lower panel; Raw data from KMD; Fig. 2)

Table 3. Discharge from Mkurumudzi River into Gazi Bay, 1966-87 (Data are from KMD)

YRS	NEM		IMLR			SEM			IMSR		NEM	
	JAN	FEB	MAR	APR	MAY	JUN	JUL	AUG	SEPT	OCT		NOV
66-77	0.30	0.29	0.08	0.51	0.95	0.56	0.14	0.09	0.05	0.19	0.45	0.30
78-80	0.05	0.04	0.03	0.20	1.18	1.59	0.04	0.27	0.05	0.25	0.35	0.30
81-87	0.06	0.07	0.08	0.07	2.51	1.48	0.48	0.19	0.26	0.22	0.25	0.30
MEAN	0.14	0.13	0.06	0.26	1.55	1.21	0.22	0.18	0.12	0.22	0.35	0.30

relationship between the total catchment area precipitation, $P = pA_c$ (where A_c is the catchment area) and the river runoff, q_r . Because of the limited amount of data a simple linear relationship between rainfall and discharge was assumed, such that $q_r = kpA_c$, where k is a retention coefficient.

Mkurumudzi River occupies 80% of the Gazi Bay catchment area, i.e. 160 km² (Table 2). The long term yearly mean discharge is 0.40 m³s⁻¹, only. With $P=7.6$ m³s⁻¹ (Table 2) the yearly mean retention coefficient is $k=0.066$. This estimate includes also the smaller Kidogoweni River, with a catchment area of 40 km². The result means that more than 93% of the precipitation over land is evaporated within the river catchment area, a figure which seems very high. Evaporation (incl. evapotranspiration), strengthened by damming of water for irrigation and other purposes is certainly high, but it's also obvious that periods of stronger rainfall are correlated with lower evaporation and relatively high runoff. By comparing Table 2 and Table 3 data, it is noted that maximum runoff in Mkurumudzi River is also delayed by about one month in comparison with the rainfall. Maximum runoff occurs in May-June while maximum rainfall occurs in April-May. In fact there are strong indications of a seasonal variation in the retention coefficient, with larger k -values during the monsoon rains.

The Pemba River, discharging into Kilindini Creek, south of Mombasa was gauged by Norconsult for a period of one year (Anon, 1975). The Pemba River has a catchment area of 905 km². The monthly discharge is shown in Table 4. With a yearly average discharge of 1.15 m³s⁻¹ and a rainfall similar to that of Tudor Creek catchment area (Table 2), it means that the retention coefficient for the Pemba River is $k=0.044$, thus even smaller than that of Gazi Bay.

Thus, the Pemba data corroborates the very small retention coefficient found in the Mkurumudzi River catchment area, and it seems

that, on average only about 5% of the coastal rainfall reaches the sea, while 95% is evaporated. In the forthcoming calculation of river discharge into Tudor Creek, the mean value, $k=0.055$ is employed. However, in the discussion various reasons are presented as to why this low figure should be used with caution.

Net sea surface heat fluxes

Weather mast data from 14 June to 28 August 1996 were used to derive the daily net sea surface heat flux, Q_{atm} (Eq 8) into Tudor Creek. Here, the incident shortwave solar radiation Q_{si} as observed by the weather mast was reduced for the sea surface albedo to obtain Q_s . The long wave back radiation, Q_b is calculated from the observed net radiation. The turbulent heat fluxes, i.e. sensible heat flux Q_h and latent heat flux, Q_e were calculated using bulk formulas according to Eqs 9-10. The albedo, A , depends strongly on the sun altitude (Payne, 1972), with a high reflection at low altitudes. The diurnal variation was not taken into account in the calculations. Instead a 4 % daily mean albedo was assumed and reduced from Q_{si} (Gill, 1982; Taylor, 2000). It means that during noon, when A is near zero, Q_{atm} (and Q_s) are overestimated by up to 50 Wm⁻² with a corresponding underestimate near sunrise and sunset. However, daily means and long-term averages should not be affected. The results, for all four components of the heat flux, including the net sea surface flux are shown in figure 8 and Table 5. The figure shows a one month series, the table indicates mean values for the whole 3 month period.

The shortwave solar radiation, Q_s entering the heat budget averages 231.9 Wm⁻² and a maximum value of 1,168 Wm⁻². If the albedo (4%, 9 Wm⁻²) is added to the average, it may be compared with the radiation data from observations at Malindi and Mombasa, shown in figure 7. It can be seen that the results from the weather mast observations, are

Table 4. River discharge (m³s⁻¹) in Pemba River, entering Kilindini Harbor, Mombasa (Data are from Norconsult; Anon, 1975)

	JAN	FEB	MAR	APR	MAY	JUN	JUL	AUG	SEP	OCT	NOV	DEC
Pemba	0.35	0.18	0.45	2.76	2.44	1.43	0.39	0.30	1.06	1.00	2.27	1.13

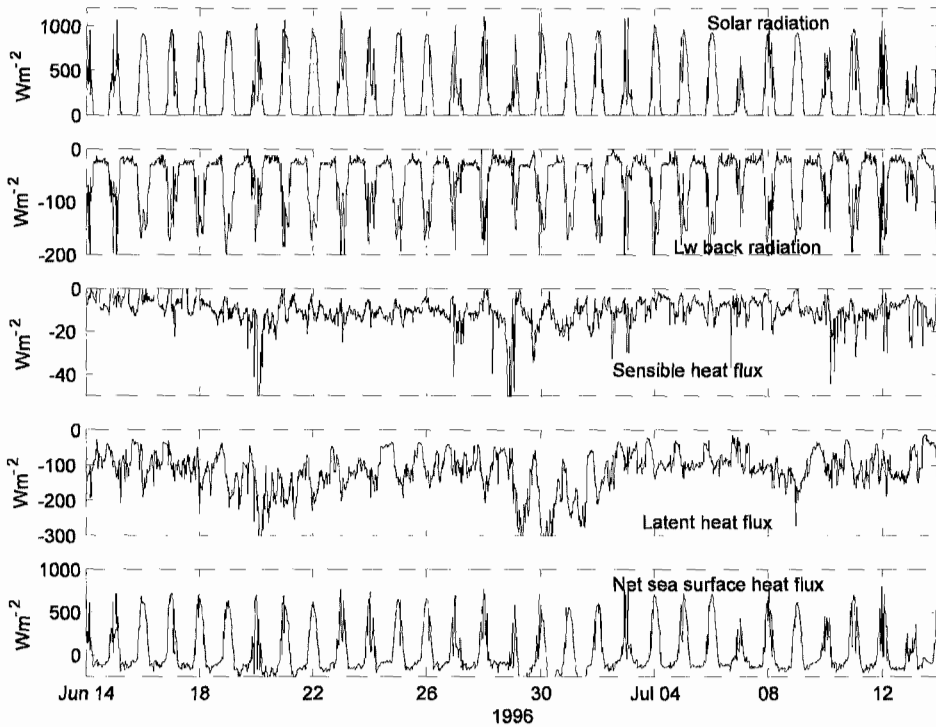


Fig. 8. Radiative and turbulent sea surface heat fluxes including the net flux, Q_{atm} calculated from weather mast data (Stn KMFRI, Mombasa) for the period from 14 June to 14 July 1996

in the upper end whereas mean Q_{si} for June-August is less than 200 Wm^{-2} . However, the impression from the data is that the cloud cover is lower than normal (Nguli, 2006). When clouds appear, Q_s is rapidly reduced (Fig. 8) but it seems as if this was rather uncommon if the whole period is considered.

The long wave back radiation, Q_b features a daily mean of -61.7 Wm^{-2} (Table 5), with variations that are otherwise typical for tropical areas (e.g. Castro *et al.*, 1994). With a few exceptions at the beginning of the observation period, the sensible heat flux, Q_h is directed out from the water, which

Table 5. Average and maximum radiative (solar radiation, Q_s and long-wave back radiation, Q_b) and turbulent heat fluxes (sensible heat flux Q_h and latent heat flux Q_e), including the net sea surface heat flux, Q_{atm} , calculated from the weather mast data, 14 June - 28 August 1996

	Q_s	Q_b	Q_h	Q_e	Q_{atm}
MAX	1168	286.2	79.5	431.4	887.6
AVERAGE	231.9	-61.7	-10.6	-117.6	41.9

is because the water temperature is higher than the air temperature during most of this period. The daily mean is 10.6 Wm^{-2} , with a maximum of 79.5 Wm^{-2} (Table 5). The latent heat, Q_e averages 117.6 Wm^{-2} , while the mean sea surface flux amounts to 42 Wm^{-2} . Similar results, with long-term monthly mean net sea surface heat fluxes of about 50 Wm^{-2} in July but 150 Wm^{-2} in January and an annual mean of about 100 Wm^{-2} are reported by Josey *et al.* (1999). Fluctuations are seen to occur within each day, and between days. Most of these are of course due to the variation in wind speed, which has a major impact on both Q_h and Q_e (see Eqs. 9-10). The latent heat flux also depends on the transfer coefficient, C_e and how it is estimated (see text, Eq. 10). The mean value of C_e for the scheme used here, amounted to 1.37×10^{-3} . This value is higher than the popular (Taylor, 2000) constant value of 1.15×10^{-3} suggested by Large and Pond (1981; 1982) but similar to the value (1.35×10^{-3}) suggested by Friehe and Schmitt (1976). The difference corresponds to a 15% lower value of Q_e , and an increase in Q_{atm} from 42 to 65 Wm^{-2} .

Seasonal temperature and salinity variations

Data from the hydrographic surveys were used to calculate average salinities and temperatures for each of the four monsoon seasons, IMLR, SEM, IMSR and NEM. The original data were averaged, vertically and divided horizontally into three different areas (upper creek, mid creek and inlet) in order to obtain consistent horizontal gradients. The results are shown in Table 6. For comparison, World Ocean Atlas (WOA01) data from the nearest offshore area (41.5E, 3.5S; depth 0-10 m) were calculated and inserted in Table 6. Offshore seasonal variations in temperature and salinity are also shown in figure 9.

Water exchange and residence times

The calculations of net freshwater discharge into Tudor Creek, q_f , according to Eq. 1c are shown in Table 7. Monthly mean rainfall over the catchment area (Table 2) is used to calculate river runoff, q_r (based on $k=0.055$) and rainfall on the creek surface, q_p . Evaporation over the creek surface, e is from figure 4, and q_e is calculated as in Table 7.

The river runoff, q_r is $0.5-3.5 \text{ m}^3\text{s}^{-1}$ during the rain seasons, but q_r is negative, up to $-1.45 \text{ m}^3\text{s}^{-1}$ during the dry NEM. Because the IMLR and the NEM were clearly dominated by either positive or negative freshwater supply, these two periods were selected for calculation of water exchange; the response to river runoff during these seasons is also more clear during these seasons than during the other two (cf Table 6).

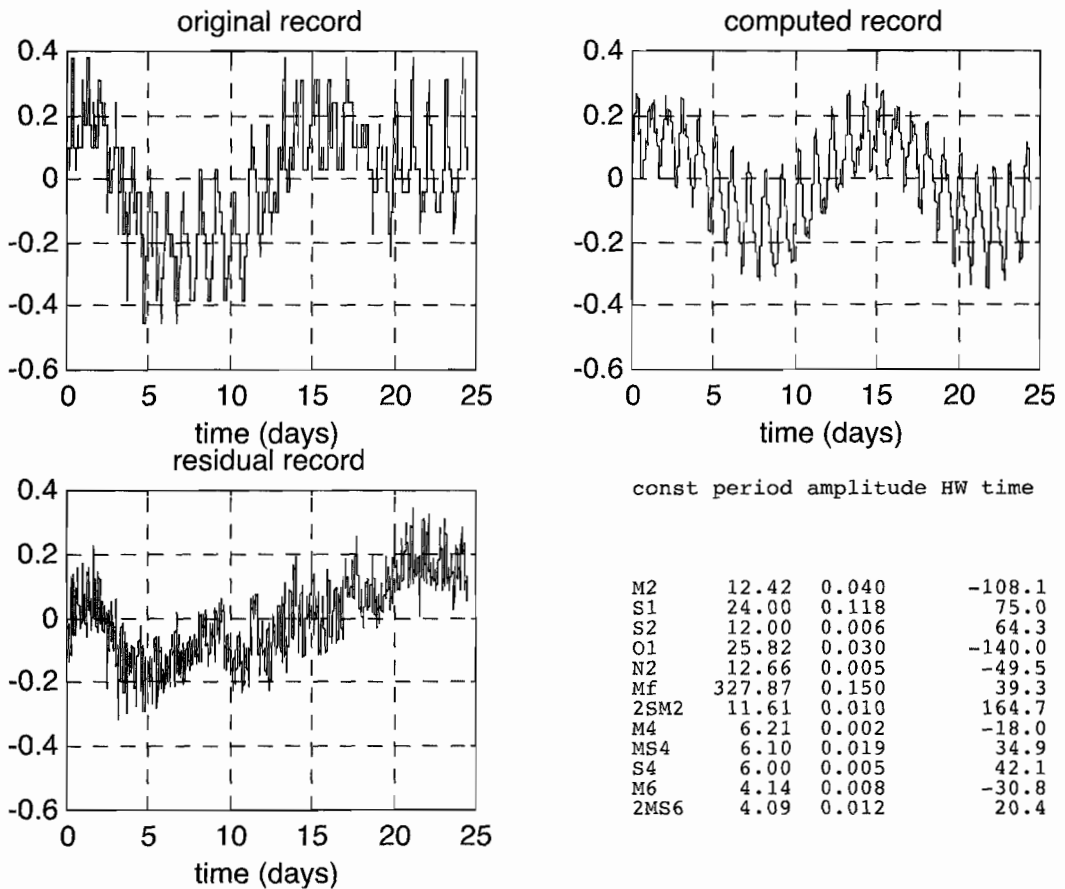


Fig. 9. Harmonic analysis of temperatures, showing original and computed records, including a table giving the amplitudes ($^{\circ}\text{C}$) of different harmonic constants. Data are from Tudor Creek, St MT2, 2-26 October 1998 (Fig. 2)

Table 6. Depth-averaged, seasonal mean salinities, S and temperatures, T in Tudor Creek for the years 1995-98

SEASON	PARAMETER	UPPER CREEK Stns I-II	MID-BAY Stns III-V	INLET: OCEAN SIDE Stn VI	OCEAN (WOA01) Lat 3.5S Long 41.5E
IMLR	S; T	24.86; 30.41	32.98; 28.86	34.76; 28.57	34.8; 28.5
SEM	S; T	35.72; 27.24	35.57; 25.92	35.45; 24.94	35.2; 25.0
IMSR	S; T	35.28; 28.72	35.31; 28.24	35.20; 27.53	35.3; 26.7
NEM	S; T	35.94; 31.67	35.93; 30.25	35.67; 29.01	35.2; 27.8

Table 7. Freshwater budget for Tudor Creek, based on long term monthly mean rainfall and evaporation in the catchment area (mm/month). River runoff, $q_r = kP$ (m^3s^{-1}) is calculated from the catchment area rainfall P (m^3s^{-1}), with $k = 0.055$. Contributions to the freshwater budget by rainfall and evaporation over the creek are determined from $q_p = pA_h$ and $q_e = eA_h$ (m^3s^{-1}). $A_h = 13 \times 10^6 m^2$

	JAN	FEB	MAR	APR	MAY	JUN	JUL	AUG	SEP	OCT	NOV	DEC	AVE
Catchm rain, p	24.4	14.8	61.4	183	260	89.9	78.4	68	58.2	135.5	109.2	72	96.2
Evaporation, e	210	203	221	184	155	144	138	158	178	197	188	191	180.6
Area rainfall, P	4.71	2.85	11.9	35.3	50.2	17.4	15.1	13.1	11.2	26.2	21.1	13.9	18.6
River runoff, q_r	0.26	0.16	0.65	1.94	2.76	0.95	0.83	0.72	0.62	1.43	1.16	0.76	1.02
Precipitation, q_p	0.19	0.11	0.47	1.40	2.00	0.69	0.60	0.53	0.45	1.04	0.84	0.56	0.74
Evaporation, q_e	1.65	1.70	1.73	1.49	1.22	1.17	1.08	1.24	1.44	1.54	1.52	1.50	1.50
Net fw flux, q_f	-1.20	-1.45	-0.61	1.85	3.54	0.47	0.35	0.01	-0.37	0.93	0.48	-0.18	0.26

Table 8 shows the results from calculations of water exchange, q_o , following Eq. 2. The salinities are taken from Table 6 data, averaged to give an integrated mean salinity, S_i for the whole volume of the creek. S_o is taken as the salinity at Stn VI in the outer part of the inlet (Fig. 2). The water exchange amounts to 182 and $25 m^3s^{-1}$, respectively and the corresponding residence times, T_r are 3.8 and 2.5 days (Eq. 5), lower during the NEM. If

Table 8. Water exchange, q_o in Tudor Creek, based on salt conservation. The mean salinity, S_i is an average of data from all stations (I-VI), whereas the "ocean" salinity S_o is represented by data from the inlet station (VI). T_r is the residence time

	S_o	S_i	ΔS	q_o m^3s^{-1}	q_r m^3s^{-1}	T_r , days
IMLR	34.76	32.17	2.59	2.01	25.0	25
SEM	35.45	35.59	-0.14	-0.18	—	—
IMSR	35.20	35.31	-0.11	-0.70	—	—
NEM	35.67	35.93	-0.26	-1.32	182.4	3.8

these results were correct, water exchange is much less efficient during the IMLR than during the NEM, which is of course not possible. However, as pointed out, the results are strongly dependent on the k -value, whereas k is likely to be strongly underestimated during periods of high rainfall. This makes estimates for the IMLR season more sensitive than estimates for the dry NEM period. Therefore, too, it is likely that results from the NEM are less unreliable. A larger retention coefficient, $k=0.25$ was tested by Nguli (2006). Then, during the IMLR, q_f would increase to about $10 m^3s^{-1}$ (instead of $2.7 m^3s^{-1}$) with a correspondingly reduced difference in water exchange and residence times between IMLR and NEM. However, at present, we are not able to determine a rainfall dependent k with a high enough accuracy to be used for determination of seasonally variable discharge in small rivers. The general conclusion, therefore, is that salinity is not a suitable tracer for calculations of water exchange in tropical areas with highly variable rainfall. The

net freshwater supply is too low in general and too variable. Continuous observations of the river runoff could be determined, but only at considerable expense. At present, establishment of useful rating curves cannot either be satisfactorily worked out.

Therefore, as an alternative to using salinity and freshwater supply for calculations of water exchange, the temperature observations and estimates of the sea surface heat fluxes were employed (Eq. 7). Estimates of net sea surface heat flux, Q_{atm} (on a seasonal time scale) were adapted from global ocean data shown in Josey *et al.* (1999). The results of these calculations are shown in Table 9. Although the estimates of Q_{atm} must be regarded as very coarse, particularly because of uncertainties in the estimates of the latent heat flux (Taylor, 2000), the results show a surprisingly high degree of conformity, where water exchange, as expected is similar during all seasons; q_o is between 278 - 314 m^3s^{-1} , with corresponding residence times, T_r of between 2.2-2.5 days.

Table 9. Water exchange, q_o in Tudor Creek, based on heat conservation. The mean temperature, T_i is an average of data from all stations (I-VI), whereas the "ocean" temperature T_o is represented by data from the inlet station (VI). T_r is the residence time

	T_o	T_i	ΔT	Q_{atm} , Wm^{-2}	q_o , m^3s^{-1}	T_r , days
IMLR	28.57	29.06	0.49	50	314	2.2
SEM	24.94	26.05	1.11	100	278	2.5
IMSR	27.53	28.29	0.76	75	305	2.3
NEM	29.01	30.55	1.54	150	301	2.3

Therefore, it can be assumed that for the Tudor Creek waters including its inlet channel, the residence time, T_r is 2-3 days. However, because the volume of the inlet occupies as much as 60% of the total volume (on average), an estimate for the bay waters alone will become higher. In addition, it is here assumed that exchange takes place with waters right outside the creek (at the oceanic side of the inlet; Stn VI), and not with the open ocean waters. The efficiency of the open ocean circulation to carry away the creek waters, once they appear outside the reef, is also of

importance for the water exchange. A slow removal gives longer residence times. Norconsult (Anon, 1975) studied the efficiency of exchange with the ocean waters on the basis of drifters released in the approaches to Mombasa. As expected, a water parcel that reaches a few km outside the reef will be rapidly removed by the East African Coastal Current. There is only a short period (from January to March) when the coastal current is weak (Schott *et al.*, 1990) and during which we may expect a slightly less efficient exchange. According to Norconsult (Anon, 1975) it may even reverse at the coast. However, as a rule of thumb, it is concluded that the residence time for the creek waters compared to the open ocean (outside the reef) is 3 - 5 days. The lower estimate includes the waters of the inlet, the upper estimate is for the bay waters. In addition there is a considerable difference between periods of neap and spring, which can not be evaluated from the present data. The tidal flow drives the diffusive exchange, with a ratio in tidal flow between peak neap and spring of 3/8. Therefore, during neap periods the residence time is about twice as long as during spring. The latter ratio applies because the residence times are shorter than the periods of neap and spring, respectively. Figure 9, showing results from temperature harmonic analysis of data from the tide gauge station MT2 (Fig. 2) position in the mid bay area, offers a nice illustration to the difference in exchange. During spring tide, the basin temperatures are lower by about 0.3°C, as indicated in the harmonic analysis table by the fortnightly component M_f for which the amplitude is 0.15°C. This is due to stronger water exchange during spring. The oceanic temperatures are 1-2 degrees lower than the bay temperatures, judging from corresponding data at Stn MT1. There is also a difference in the daily temperature range from about 0.3°C during spring to about 0.2°C during neap. However, this difference is obscured by diurnal heating and cooling (indicated by the component $S_1=24$ hrs) which dominates the diurnal temperature variations (see also Nguli, 2006).

CONCLUSIONS

The focus of this paper is on determination of water exchange from salt and heat budgets. Hydrographic

surveys were carried out for this purpose to give the mean seasonal salinity and temperature distribution. However, the inputs of freshwater and heat needed in order to use the conservation equations, were not directly observed but had to be estimated from other sources, including local (KMD) data on rainfall and evaporation and global web data for the sea surface heat fluxes, respectively.

Serious problems were experienced in establishing reliable estimates of the river discharge into the creek. Application of a constant retention coefficient, $k=0.055$, relating rainfall to discharge through a linear rating curve, was not successful, particularly not during periods of high rainfall, such as during the IMLR. The retention coefficient was far too small to fit with the low bay salinities. This is shown in this paper, but was clear also from comparing gauging data in Mkurumudzi River with independent measurements of runoff (Kitheka, 1997).

As aforementioned, there are also several reasons why a single value for k will not suffice. First, k depends on the rainfall, where larger rainfall is likely to give a larger k and a non-linear rating curve. Thus the rain seasons should have a larger k , and the dry seasons a smaller. Secondly, a larger catchment area is expected to give a smaller k . The Tana River, the largest river in Kenya, has a k of approx. 0.07 (Olago, pers.comm), a value which is probably well established. Finally, irrigation and damming have a large local impact on how much of the rainfall reaches the sea as river discharge. At present, determination of runoff from rainfall does not seem an appropriate method. This also hindered obtaining reliable estimates on water exchange based on salinity observations. At least some of the seasonal rivers entering the southern Kenya coast should have permanent gauging installed. On the other hand the efforts gave some insight in the coastal meteorology with updated figures on monthly means of evaporation, rainfall and incident solar radiation. These data can be compared to an earlier review (McClanahan, 1988).

In conclusion, although the most common way to estimate water residence time in estuaries is by using salt conservation, particularly when the freshwater discharge is large, an alternative method

is to use heat conservation. In our case, introduction of a heat budget for the Tudor Creek was found to be a much better approach. The reasons include the fact that the seasonal variations in sea surface heat flux, Q_{am} are strong and bring about a correspondingly strong temperature difference, ΔT whereas the net freshwater supply, q_f which is the corresponding signal in the salt equation, is weaker, more variable and almost unpredictable. Using the heat equation (temperature observations and global ocean sea surface heat fluxes) for Tudor Creek as a whole, including the inlet channel, the water residence time was found to be of the order of 3 days, but 5 days for the waters inside the inlet. Harmonic analysis of temperature data indicated a considerable (factor two) difference in residence time between spring and neap.

REFERENCES

- Anon (1975) Mombasa water pollution and waste disposal study: Report to the Ministry of Local Government, Nairobi Vol. VI. Norconsult, A.S. 104 pp.
- Anon (1996a) Kenya Meteorological Department (KMD), *Climatologic Statistics*.
- Anon (1996b) Kenya Meteorological Department (KMD). *Water discharge at gauging station 3KDA on Mukurumuji River between 1961 and 1987*.
- Anon (1997) Kenya Meteorological Department (KMD), *Climatologic Statistics*.
- Arons, A. B. and Stommel, H. (1951) A mixing-length theory of tidal flushing. *Transactions, American Geophysical Union* **32**, 419-421.
- Castro, R., Lavin, M.F and Ripa, P. (1994). Seasonal heat balance in the Gulf of California, *Journal of Geophysical Research*, **99**, C2, pp 3249-3261.
- Friehe, C.A. and Schmitt, K.F. (1976) Parameterization of air air-sea interface fluxes of sensible heat and moisture by the bulk aerodynamic formulas. *J. Phys. Oceanogr.* **6**: 801-809.
- Gill, A. E. (1982) *Atmosphere-Ocean Dynamics*. Academic Press, Inc. San Diego. 662pp.
- Josey, S.A., Kent, E. C. and Taylor, P.K. (1999) New insights into the ocean heat budget closure problem from analysis of the SOC air sea flux climatology. *J. Clim.* **12**: 2856-80.
- Kitheka, J. (1997) Coastal Tidally-driven circulation and role of water exchange in the linkage between tropical coastal ecosystems. *Est. Coast. Shelf Sci.* **45**, 177-187.
- Knudsen, M. (1899) De hydrografiske forhold i de danske farvande indenfor Skagen 1894-1898.

- Beretning fra Kommissionen för videnskablig undersögelse av de danske Farvande. Copenhagen, Denmark Band **2(2)**:19-79.
- Large, W.G. and Pond, S. (1981) Open ocean momentum flux measurements in moderate to strong winds, *J. Phys. Oceanogr.* **11**: 324-336.
- Large, W.G. and Pond, S. (1982) Sensible and latent heat flux measurements over the ocean. *J. Phys. Oceanogr.* **12**, 464-482.
- Magori C. (1998) Tidal propagation and water exchange in Mtwapa creek, Kenya. MSc Thesis Ser. B70. Gothenburg University. 26pp.
- McClanahan, T.R. (1988) Seasonality in the Eastern Africa's coastal water. *Mar. Ecol. Progr. Ser.* **44**: 191-199.
- Mohanty, U.C. and Mohan Kumar, N. (1990). A study of surface marine boundary layer fluxes over the Indian Seas during different epochs of Asian Summer Monsoon. *Atmos. Environ.*, **24A**, 823-828.
- Mohanty, U.C and Ramesh, K. J. (1996). Certain seasonal characteristic features of oceanic heat budget components over the Indian Seas in relation to the summer monsoon activity over India. *International Journal of Climatology.*, **16**, 243-264.
- Nguli, M.M. (1994) Water exchange and channel friction related to tidal flow in Tudor creek, Kenya coast, Western Indian Ocean. MSc Thesis. Gothenburg University, Sweden 32 pp.
- Nguli, M.M. (2006) Water exchange and circulation in selected Kenyan Creeks. PhD Thesis. University of Dar es Salaam, Tanzania. 251 pp.
- Nunes Vaz, R.A., Lennon, G.W and De Silva Samarasinghe, J.R. (1989) The negative role of turbulence in estuarine mass transport. *Est. Coast. Shelf Sci.* **28**: 361-377.
- Odido, M.O. (1994) Tidal dynamics of Tudor Creek. Mombasa Kenya, MSc Thesis. Gothenburg University, Sweden. 30 pp.
- Payne, R.E. (1972) Albedo of the sea surface. *Journal of the Atmospheric Sciences* **29**: 959-970.
- Pugh, D.T. (1979) Sea level at Aldabra Atoll, Mombasa and Mahe. Western Equatorial Indian Ocean, related to tides, meteorology and circulation. *Deep-Sea Res.* **26**: 237-258.
- Schott, F., Swallow, J.C. and Fieux M. (1990) The Somali current at the equator: annual cycle of currents and transport in the upper 1000m and connection to the neighbouring latitudes. *Deep-sea Res.* **37**: 1825-1990
- Stommel, H. and Farmer, H.G. (1953) Control of salinity in an estuary by transition. *J.Mar. Res.* **12**: 13-20.
- Taylor, P.K. (2000) Intercomparison and validation of ocean-atmosphere energy flux fields. By members of WGASF, ed. P.K. Taylor. SCOR WG 110. 306 pp.